Buckling of hybrid orthotropic rectangular plates with one edge partially restrained against rotation and subjected to uniform compression strain loading

Wael F. Ragheb
Structural Engg. Dept., Faculty of Engg., Alexandria University, Alexandria, Egypt 21544

This paper presents an analytical stability model to predict the buckling strength of an orthotropic hybrid rectangular plate. The plate is considered to be a hybrid of two orthotropic materials and is subjected to in-plane uniform uniaxial compression strain loading. The loaded edges of the plate are considered to be simply supported while one of the unloaded edges is free and the other edge is considered to be elastically restrained against rotation. Based on the stability model presented, the parameters governing the buckling behavior of the hybrid plate are identified. A parametric study is presented to investigate the effect of each of the parameters on the overall buckling strength of the plate. The study results show that providing a stiffer material part near the rotationally restrained edge generally provides higher overall buckling capacity than providing it near the free edge. The peak high in plate buckling capacity does not occur with the plate totally made of the stiffer material. Providing the plate with a stiffer material at its edge might result in a decrease in its buckling capacity.

يقدم هذا البحث نموذج تحليلي لحساب مقاومة الانبعاج للوح مستطيل هجين متباين الخواص. واللوح الذي تم تناوله هو هجين من نوعين من المواد ذات الخواص المتباينة و معرض لانفعال ضغط محوري موزع بانتظام. وهذا اللوح يرتكز ارتكازا بسيطا عند حافتيه المحملتين بينما أحد حافتيه الغير محملتين ممنوعة جزئيا من الدوران و الحافة الأخرى حرة. وبناء على النموذج التحليلي الذي تم تقديمه تم تحديد المعاملات التي تحكم سلوك الانبعاج لمثل هذا اللوح. وتم كذلك تقديم دراسة تحليلية لتحديد مدي تأثير هذه المعاملات على سلوك الانبعاج الكلى للوح. و لقد بينت هذه الدراسة أن وجود مادة أكثر جسائة عند الطرف الممنوع جزئيا من الدوران يؤدي زيادة كبيرة في مقاومة الانبعاج الكلية للوح أكثر من وجود هذا الجزء عند الطرف الحر. ولقد بينت الدراسة أن مقاومة الانبعاج القصوى لا تحدث بالضرورة عندما يكون اللوح بالكامل من المادة الأكثر جسائة كما و أن وضع مادة أكثر جسائة عند الطرف الحر قد تؤدى الى تقليل مقاومة اللوح للانبعاج بدلا من زيادتها.

Keywords: Buckling, Orthotropic plates, FRP, Composites, Hybrid

1. Introduction

With the increase of use of composite materials in structural applications, there has come a need to develop mathematical models to analysis the behavior of such materials, especially their buckling behavior. Fiber Reinforced Polymers (FRP) are classified as orthotropic materials that have relatively high strength to stiffness ratio in the direction of the fibers that makes them more likely to fail in buckling. FRP structural profiles such as angle, channels, and I-sections are basically assemblies of thin flat plates and they are typically manufactured using the pultrusion process [1]. Therefore, buckling analysis of such shapes can be done by modeling their flanges or webs individually as orthotropic composite plates. For example, the problem of the local buckling of the compression flange of an I-beam loaded in bending can be modeled as a rectangular plate whose two loaded edges are simply supported, one of the unloaded edges is free, and other end is elastically restrained against rotation, which represents the influence of the web on the flange [2-4].

The stability problem of a rectangular orthotropic plate that is subjected to uniform compression stresses has been discussed in numerous publications [5-9]. However, little work was reported on the solution of the same problem but with rotationally restrained edges. Bank and Yin [10] presented an analytical solution for the buckling of a rectangular orthotropic plate that was subjected to uniform uniaxial compression and simply supported on the loaded edges while one of the unloaded edges was free and

the other edge was elastically restrained against rotation. Qiao and Zou [3] presented an explicit elastic stability solution for the same problem. Mittelstedt [11] presented an analytical investigation for the buckling of symmetrically laminated rectangular orthotropic plates under uniaxial compression in which the loaded edges were considered to be simply supported while the unloaded ones were considered to be elastically restrained against rotation.

While these models are capable of dealing with the problem of a hybrid laminated plate that has several layers of different materials through its thickness, none of them covers the case when the plate is a hybrid of more than one material along its width. For example, the local buckling of the compression flange of an FRP I- beam that is a hybrid of more than one type of fiber along the width of its flange can not be modeled using any of the currently available models. In such case, it is important to note that the compression flange of a non-hybrid I-beam loaded in bending is uniformly strained and therefore it is also uniformly stressed. However, that is not the case when the compression flange is a hybrid of two materials. In such case, the compression flange of the beam will be uniformly strained but not uniformly stressed, which has to be taken into consideration while developing a stability model for it.

The present contribution is devoted to the development of an analytical model to predict the buckling strength of an orthotropic rectangular plate that is a hybrid of two materials and subjected to in-plane uniform uniaxial compression strain. The loaded edges of the plate were considered to be simply supported while one of the unloaded ones was considered to be free and the other edge was considered to be rotationally restrained. A parametric study was conducted to investigate the influence of each of the parameters of the problem on the overall buckling strength of the plate.

2. Description of the problem

Fig.1 illustrates the current problem of an orthotropic plate that is a hybrid of two orthotropic materials, namely, A and B. Each material had the elastic properties E_x, E_y, G and υ. Note that the superscripts A and B will be used throughout the paper to refer to any of parameters of the two materials of the plate. The plate has a total width of (b), a length of (a), and a constant thickness (t). The solution is based on considering the plate as being composed of two parts (A and B) that are perfectly connected along their border line. The width of part A is considered to be ($b1$) where ($b1 = r.\ b$) and (r) is defined herein as a width ratio ($r = b1/b$). The plate was considered to be subjected to uniaxial uniform strain. Assuming that part B is subjected to a uniform compression load per unit width (N_x), the stresses acting on this part will be equal to (Nx/t). Since the strain is uniform, the stresses acting on part A will therefore be equal to (E_x^A/E_x^B). ($N_x\ \ t$). Accordingly, the load acting on part A will be equal to ($E_x^A.Nx/E_x^B$).

3. Stability analysis

The analysis is based on dealing with each part of the plate independently including its boundary conditions. Then, the continuity conditions at the border line between the two parts were considered.

3.1. Part A

The governing differential equation for the linear buckling analysis of an orthotropic plate whose axes of material orthotropy coincide with the axis of the plate, as expressed by Timoshenko and Gere [5], can be applied for part A as follows:

$$D1^A.\frac{\partial^4 w^A}{\partial x^4}+2\,D3^A\,\frac{\partial^4 w^A}{\partial x^2\partial y^2}+D2^A.\frac{\partial^4 w^A}{\partial y^4}+(N_x\,\frac{E_x{}^A}{E_x{}^B})\frac{\partial^2 w^A}{\partial x^2}=0\,, \qquad (1)$$

where:

$$D1^A=\frac{E_x{}^A.t^3}{12\,(1-\upsilon_x{}^A.\upsilon_y{}^A)}.$$

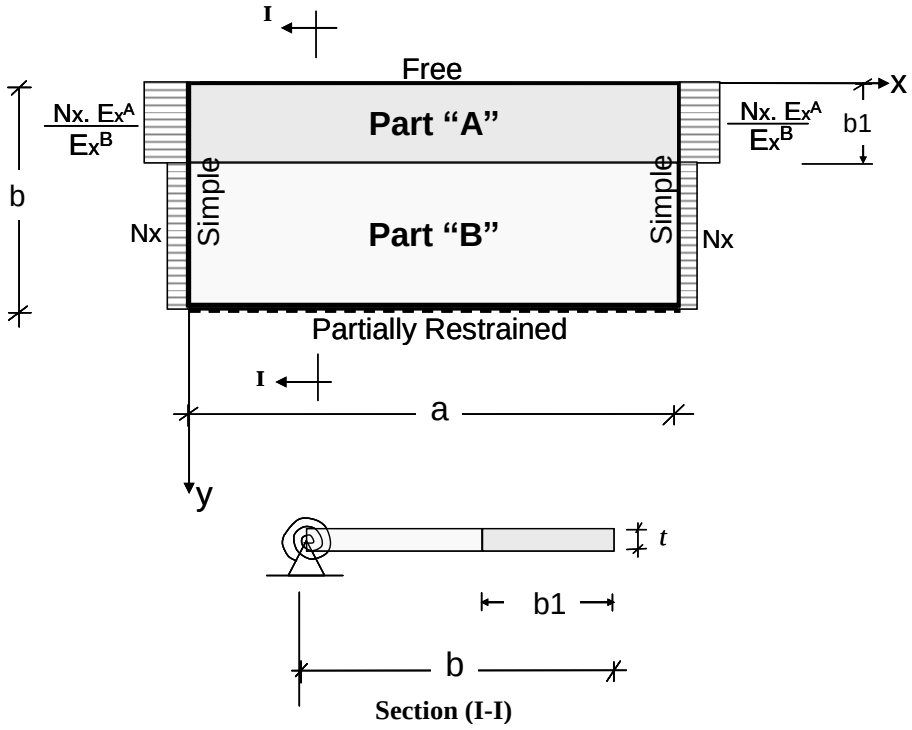

Fig. 1. An orthotropic hybrid plate with one rotationally restrained edges that is subjected to uniform strain loading.

$$D2^A = \frac{E_y{}^A . t^3}{12(1 - \upsilon_x{}^A . \upsilon_y{}^A)} .$$

$$D3^A = D1^A . \upsilon_y{}^A + \frac{G^A . t^3}{6} ,$$

where $E_x{}^A$ and $E_y{}^A$ are the moduli of elasticity in the two mutually perpendicular principal directions x and y, G^A is the in-plane shear modulus, $\upsilon_x{}^A$ and $\upsilon_y{}^A$ are the major and minor Poisson's ratios, respectively, and w is the transverse displacement of the plate due to buckling.

The boundary conditions on part A of the plate excluding the border line with part B are expressed as follows:

1. The plate is simply supported at the loaded edges and therefore the transverse displacements at (x = 0, a) must equal to zero:

$$[w^A]_{x=0,a} = 0 . \qquad (2)$$

2. The simply supported conditions at the loaded edges guarantees that the bending moment per unit length (M_x) must equal to zero and therefore:

$$[M_x]_{x=0,a} = 0$$

$$[M_x]_{x=0,a} = -\left[D1^A \frac{\partial^2 w^A}{\partial x^2} + \upsilon_x{}^A . D1^A \frac{\partial^2 w^A}{\partial y^2} \right]_{x=0,a} = 0.$$

Since the edges at x = 0 and at x = a are simply supported, the value of $\frac{\partial^2 w^A}{\partial y^2}$ must equal zero and therefore:

$$\left[\frac{\partial^2 w^A}{\partial x^2} \right]_{x=0,a} = 0 . \qquad (3)$$

3. The bending moment per unit length (M_y) at the free edge must be equal to zero and hence:

$$[M_y]_{y=0} = 0 .$$

$$\left[M_y\right]_{y=0} = -\left[D2^A \frac{\partial^2 w^A}{\partial y^2} + \upsilon_x{}^A . D2^A \frac{\partial^2 w^A}{\partial x^2} \right]_{y=0} = 0.$$

Dividing both sides by $(-D2^A)$:

$$\left[\frac{\partial^2 w^A}{\partial y^2} + \upsilon_x{}^A \frac{\partial^2 w^A}{\partial x^2} \right]_{y=0} = 0 \ . \qquad (4)$$

4. The magnitude of the shearing forces per unit length (V_y) at the free edge of the plate must be equal to zero. Timoshenko and Gere [5] showed that the magnitude of the shearing forces is equal to the shearing force per unit length (Q_y) plus the equivalent shearing forces resulting from of the twisting moment M_{xy} and therefore:

$$\left[V_y\right]_{y=0} = \left[Q_y + \frac{\partial M_{xy}}{\partial x} \right]_{y=0} = 0$$

$$\left[D2^A \frac{\partial^3 w^A}{\partial y^3} + (2\,D3^A - \upsilon_x{}^A . D2^A) \frac{\partial^3 w^A}{\partial x^2\, \partial y} \right]_{y=0} = 0.$$

Dividing both sides by $D2^A$

$$\left[\frac{\partial^3 w^A}{\partial y^3} + (2 \frac{D3^A}{D2^A} - \upsilon_x{}^A) \frac{\partial^3 w^A}{\partial x^2\, \partial y} \right]_{y=0} = 0 . \qquad (5)$$

3.2. Part B

The governing differential equation for part B is similar to that of part A except that load acting on the plate will be replaced by (N_x) and therefore it will take the form:

$$D1^B . \frac{\partial^4 w^B}{\partial x^4} + 2\,D3^B \frac{\partial^4 w^B}{\partial x^2 \partial y^2} + D2^B . \frac{\partial^4 w^B}{\partial y^4} + N_x . \frac{\partial^2 w^B}{\partial x^2} = 0 , \qquad (6)$$

where

$$D1^B = \frac{Ex^B . t^3}{12\,(1 - \upsilon_x{}^B . \upsilon_y{}^B)} .$$

$$D2^B = \frac{Ey^B . t^3}{12\,(1 - \upsilon_x{}^B . \upsilon_y{}^B)} .$$

$$D3^B = D1^B . \upsilon_y{}^B + \frac{G^B . t^3}{6} .$$

The boundary conditions on the edges of part B excluding the borderline with part A are expressed as follows:

1. The simply supported conditions at the loaded edges give zero transverse displacements and therefore:

$$[w^B]_{x=0,a} = 0 . \qquad (7)$$

2. The bending moments M_x at the loaded edges are equal to zero

$$[M_x]_{x=0,a} = \left[\frac{\partial^2 w^B}{\partial x^2} \right]_{x=0,a} = 0 . \qquad (8)$$

3. The transverse displacements at the rotationally restrained edge are equal to zero:

$$[w^B]_{y=b} = 0 . \qquad (9)$$

4. The moment equilibrium at the rotationally restrained edge ($y = b$) of the plate gives the following relation [10]

$$\left[M_y - S \frac{\partial w^B}{\partial y} \right]_{y=b} = 0 . \qquad (10)$$

where (S) is the restraining moment along the rotationally restrained edge per unit length per unit rotation.

$$M_y = -\left[D2^B \frac{\partial^2 w^B}{\partial y^2} + \upsilon_x{}^B . D2^B \frac{\partial^2 w^B}{\partial x^2} \right].$$

Since the transverse displacements at $y = b$ are equal to zero, the value of $\frac{\partial^2 w^B}{\partial x^2}$ is equal to zero and therefore eq. (10) becomes:

$$\left[\frac{\partial^2 w^B}{\partial y^2} + \frac{S}{D2^B} . \frac{\partial w^B}{\partial y} \right]_{y=b} = 0 .$$

Introducing the dimensionless factor $R = \frac{S.b}{D2^B}$ and multiplying both sides by (b), eq. (10) becomes:

$$\left[b \frac{\partial^2 w^B}{\partial y^2} + R . \frac{\partial w^B}{\partial y} \right]_{y=b} = 0 . \quad (11)$$

The boundary conditions at border line between the two parts of the plate are:

1 –The transverse displacements from both parts of the plate become identical at the border line, i.e., at $y = b1$.

$$\left[w^A\right]_{y=b1} = \left[w^B\right]_{y=b1} . \quad (12)$$

2- The bending moments M_y from both parts of the plate become equal at the border line between the two parts:

$$\left[M_y{}^A\right]_{y=b1} = \left[M_y{}^B\right]_{y=b1}$$

$$\left[D2^A \frac{\partial^2 w^A}{\partial y^2} + D2^A . \upsilon_x{}^A \frac{\partial^2 w^A}{\partial x^2} \right]_{y=b1}$$

$$= \left[D2^B \frac{\partial^2 w^B}{\partial y^2} + D2^B . \upsilon_x{}^B \frac{\partial^2 w^B}{\partial x^2} \right]_{y=b1} . \quad (13)$$

3- Similarly, the magnitude of the shearing forces calculated from both parts are equal at the $y = b1$.

$$\left[V_y{}^A\right]_{y=b1} = \left[V_y{}^B\right]_{y=b1}$$

$$\left[D2^A \frac{\partial^3 w^A}{\partial y^3} + (2 D3^A - \upsilon_x{}^A . D2^A) \frac{\partial^3 w^A}{\partial x^2 \partial y} \right]_{y=b1}$$

$$= \left[D2^B \frac{\partial^3 w^B}{\partial y^3} + (2 D3^B - \upsilon_x{}^B . D2^B) \frac{\partial^3 w^B}{\partial x^2 \partial y} \right]_{y=b1} . \quad (14)$$

4- In order to verify the continuity of the plate at the border line between its two parts, the slope calculated from both parts must be equal and therefore,

$$\left[\frac{\partial w^A}{\partial y} \right]_{y=b1} = \left[\frac{\partial w^B}{\partial y} \right]_{y=b1} . \quad (15)$$

4. Solution of the differential equations

It is convenient to solve the differential eqs. (1 and 6) using the Levy's solution. The equations shown below give an expression for the buckling displacements w^A and w^B that satisfy the boundary conditions expressed in eqs. (2, 3, 7 and 8). Accordingly, the solution will take the following forms:

a- For part (A)

$$w^A = f^A(Y) . \sin\left(\frac{m\pi x}{a} \right) . \quad (16)$$

b- For part (B)

$$w^B = f^B(Y) . \sin\left(\frac{m\pi x}{a} \right) , \quad (17)$$

where

$$Y = \frac{y}{b} .$$

Substituting with eqs. (16 and 17) into the differential eqs. (1 and 6), respectively, they become:

a- For part (A)

$$\frac{\partial^4 f^A}{\partial Y^4} - 2\left(\frac{D3^A}{D2^A} \right)\left(\frac{b}{a} \right)^2 \left(m^2 \pi^2 \right) \frac{\partial^2 f^A}{\partial Y^2}$$

$$+ \left[\left(\frac{D1^A}{D2^A} \right)\left(\frac{b}{a} \right)^4 \left(m^4 \pi^4 \right) - K_x{}^A . \left(m^2 \pi^4 \right)\left(\frac{b}{a} \right)^2 \right] f^A = 0 , \quad (18)$$

Where, $K_x{}^A$ is a dimensionless factor that is given from

$$K_x{}^A = \left(N_x \frac{E_x{}^A}{E_x{}^B} \right) \frac{b^2}{D2^A . \pi^2} .$$

b- For part (B)

$$\frac{\partial^4 f^B}{\partial Y^4} - 2\left(\frac{D3^B}{D2^B}\right)\left(\frac{b}{a}\right)^2 \left(m^2 \pi^2\right) \frac{\partial^2 f^B}{\partial Y^2} + \left[\left(\frac{D1^B}{D2^B}\right)\left(\frac{b}{a}\right)^4 \left(m^4 \pi^4\right) - K_x{}^B . \left(m^2 \pi^4\right) \left(\frac{b}{a}\right)^2 \right] f^B = 0 . \quad (19)$$

where, $K_x{}^B$ is a dimensionless factor that is given from:

$$K_x{}^B = (N_x) \frac{b^2}{D2^B . \pi^2} .$$

The boundary conditions expressed above in eqs. (4, 5, 9, 11 and 12 through 15) are rewritten below in view of the solutions of the governing differential equations, i.e., eqs. (16 and 17). Accordingly, these boundary conditions will be:

$$1\text{-} \left[\frac{\partial^2 f^A}{\partial Y^2} - \left(v_x{}^A \left(\frac{b}{a}\right)^2 m^2 \pi^2 \right) f^A \right]_{Y=0} = 0 . \quad (20)$$

$$2\text{-} \left[\frac{\partial^3 f^A}{\partial Y^3} - \left((2\frac{D3^A}{D2^A} - v_x) \left(\frac{b}{a}\right)^2 m^2 \pi^2 \right) \frac{\partial f^A}{\partial Y} \right]_{Y=0} = 0 . \quad (21)$$

$$3\text{-} \left[f^B \right]_{Y=1} = 0 . \quad (22)$$

$$4\text{-} \left[\frac{\partial^2 f^B}{\partial Y^2} + R \frac{\partial f^B}{\partial Y} \right]_{Y=1} = 0 . \quad (23)$$

$$5\text{-} \left[f^A \right]_{Y=r} = \left[f^B \right]_{Y=r} . \quad (24)$$

$$6\text{-} \left[\left(\frac{D2^A}{D2^B}\right) \frac{\partial^2 f^A}{\partial Y^2} + \left(\frac{D2^A}{D2^B}\right) . v_x{}^A . \left(\frac{b}{a}\right)^2 (-m^2 \pi^2) f^A \right]_{Y=r} = \left[\frac{\partial^2 f^B}{\partial Y^2} + v_x{}^B \left(\frac{b}{a}\right)^2 (-m^2 \pi^2) f^B \right]_{Y=r} . \quad (25)$$

$$7\text{-} \left[\begin{array}{l} \left(\frac{D2^A}{D2^B}\right) \frac{\partial^3 f^A}{\partial Y^3} + \left(2 \left(\frac{D3^A}{D2^A}\right) \left(\frac{D2^A}{D2^B}\right) - v_x{}^A . \left(\frac{D2^A}{D2^B}\right) \right) \\ \left(\frac{b}{a}\right)^2 (-m^2 \pi^2) \frac{\partial f^A}{\partial Y} \end{array} \right]_{Y=r} = \left[\frac{\partial^3 f^B}{\partial Y^3} + (2 \left(\frac{D3^B}{D2^B}\right) - v_x{}^B) \left(\frac{b}{a}\right)^2 (-m^2 \pi^2) \frac{\partial f^B}{\partial Y} \right]_{Y=r} . \quad (26)$$

$$8\text{-} \left[\frac{\partial f^A}{\partial Y} \right]_{Y=r} = \left[\frac{\partial f^B}{\partial Y} \right]_{Y=r} . \quad (27)$$

Rewriting the governing differential eqs. (18 and 19) in the following simplified form:

$$\frac{\partial^4 f^A}{\partial Y^4} - \alpha_A \frac{\partial^2 f^A}{\partial Y^2} + \beta_A . f^A = 0 . \quad (28)$$

$$\frac{\partial^4 f^B}{\partial Y^4} - \alpha_B \frac{\partial^2 f^B}{\partial Y^2} + \beta_B . f^B = 0 . \quad (29)$$

where,

$$\alpha_A = 2\left(\frac{D3^A}{D2^A}\right)\left(\frac{b}{a}\right)^2 \left(m^2 \pi^2\right).$$

$$\beta_A = \left(\frac{D1^A}{D2^A}\right)\left(\frac{b}{a}\right)^4 \left(m^4 \pi^4\right) - K_x{}^A . \left(m^2 \pi^4\right) \left(\frac{b}{a}\right)^2 .$$

$$\alpha_B = 2\left(\frac{D3^B}{D2^B}\right)\left(\frac{b}{a}\right)^2 \left(m^2 \pi^2\right)$$

$$\beta_B = \left(\frac{D1^B}{D2^B}\right)\left(\frac{b}{a}\right)^4 \left(m^4 \pi^4\right) - K_x{}^B . \left(m^2 \pi^4\right) \left(\frac{b}{a}\right)^2 .$$

The solution of the differential equations above will take the following form:

$$f^A = C1\,.\,e^{\lambda 1A.(Y)} + C2\,.\,e^{-\lambda 1A.(Y)} + C3.\sin(\lambda 2A.(Y)) + C4\,.\cos(\lambda 2A.(Y)), \quad (30)$$

where

$$\lambda 1A = 0.5\sqrt{2\alpha_A + 2\sqrt{{\alpha_A}^2 - 4\beta_A}}$$

$$\lambda 2A = 0.5\sqrt{-2\alpha_A + 2\sqrt{{\alpha_A}^2 - 4\beta_A}}$$

$$f^B = C5\,.\,e^{\lambda 1B.(Y)} + C6\,.\,e^{-\lambda 1B.(Y)} + C7.\sin(\lambda 2B.(Y)) + C8\,.\cos(\lambda 2B.(Y)), \quad (31)$$

where:

$$\lambda 1B = 0.5\sqrt{2\alpha_B + 2\sqrt{{\alpha_B}^2 - 4\beta_B}}\,.$$

$$\lambda 2B = 0.5\sqrt{-2\alpha_B + 2\sqrt{{\alpha_B}^2 - 4\beta_B}}\,.$$

The boundary conditions related to the y-coordinates of the plate, i.e., eqs. (20 through 27) were used to get eight equations in terms of the constants C1 through C8. Details of these equations can be found in Appendix I. This system of equations can be organized in the following matrix form:

$$[\eta].[C]=[0]$$

$$\begin{bmatrix} \eta_{11} & \eta_{12} & 0 & \eta_{14} & 0 & 0 & 0 & 0 \\ \eta_{21} & \eta_{22} & \eta_{23} & 0 & 0 & 0 & 0 & 0 \\ 0 & 0 & 0 & 0 & \eta_{35} & \eta_{36} & \eta_{37} & \eta_{38} \\ 0 & 0 & 0 & 0 & \eta_{45} & \eta_{46} & \eta_{47} & \eta_{48} \\ \eta_{51} & \eta_{52} & \eta_{53} & \eta_{54} & \eta_{55} & \eta_{56} & \eta_{57} & \eta_{58} \\ \eta_{61} & \eta_{62} & \eta_{63} & \eta_{64} & \eta_{65} & \eta_{66} & \eta_{67} & \eta_{68} \\ \eta_{71} & \eta_{72} & \eta_{73} & \eta_{74} & \eta_{75} & \eta_{76} & \eta_{77} & \eta_{78} \\ \eta_{81} & \eta_{82} & \eta_{83} & \eta_{84} & \eta_{85} & \eta_{86} & \eta_{87} & \eta_{88} \end{bmatrix} \cdot \begin{bmatrix} C1 \\ C2 \\ C3 \\ C4 \\ C5 \\ C6 \\ C7 \\ C8 \end{bmatrix} = \begin{bmatrix} 0 \\ 0 \\ 0 \\ 0 \\ 0 \\ 0 \\ 0 \\ 0 \end{bmatrix}$$

The nontrivial solution of this system of equation can be obtained by setting the determinant of the (η) matrix to zero. Therefore, for a given plate geometry (a, b, r, t), plate stiffness ($D1^A$, $D2^A$, $D3^A$, $D1^B$, $D2^B$, $D3^B$, $\upsilon_x{}^A$, $\upsilon_x{}^B$, R), and the mode number m, the buckling coefficient $K_x{}^A$ can be obtained. Note that $K_x{}^B$ can be easily obtained as it is related to the value of $K_x{}^A$.

5. Parametric study

In view of the analytical model presented, it is obvious that the dimensionless parameters that govern the buckling behavior of the plate are $(D1/D2)^A$, $(D1/D2)^B$, $(D2/D3)^A$, $(D2/D3)^B$, $(D2^A/D2^B)$, $\upsilon_x{}^A$, $\upsilon_x{}^B$, $K_x{}^A$, $K_x{}^B$, r, (a/b), and R. Since the values of $K_x{}^A$ and $K_x{}^B$ are related to each others, it was necessary and more convenient to combine them into a single parameters by introducing the dimensionless parameter $K_x{}^*$. This parameter reflects the overall buckling capacity of the plate and it is defined as follows:

$$\mathrm{K}_{\mathrm{x}}^{*} = \frac{Nx_{av}\,.\,b^2}{\pi^2\,.\,D2_{av}},$$

Where

$$Nx_{av} = [N_x\,\frac{E_x{}^A}{E_x{}^B}\,.\,r + N_x\,.\,(1 - r)].$$

$$D2_{av} = (D2^A + D2^B)\,/\,2.$$

A computer program was prepared to solve the problem where the parameters mentioned above were set as the inputs of the program and the value of $K_x{}^*$ was calculated by the program as an output. The program was used to conduct a parametric study to investigate the effect of each of the parameters on the buckling strength of the plate.

6. Study results and discussion

The main objective of the parametric study was to investigate the effect of the relative stiffness of the materials of the two parts of the plate, as well as, their relative location on the overall buckling strength of the plate. The relative material stiffness and location are mainly describes by the parameters $(D1/D2)^A$, $(D1/D2)^B$, $(D2^A/D2^B)$, and (r).

6.1. Typical buckling curves

Fig. 2 through fig. 4 show the buckling curves of an orthotropic plate that is a hybrid of two materials. The curves are plotted for multiple values of the parameters mentioned above. Fig. 2 shows the buckling curves for multiple values of *R*. It is obvious from the values of *Kx** shown in figure that providing the material with the greater $(D1/D2)$, i.e., the stiffer material, near the rotationally restrained edge resulted in higher *Kx** than providing it near the free edge. Fig. 3 shows similar buckling curves but with multiple values of $(D1/D2)^B$ and $(D1/D2)^A$. It is evident that increasing $(D1/D2)^B$ results in significant increases in *Kx**, which was not relatively the same when the value of $(D1/D2)^A$ was increased. It can be noticed from fig. 4-i that the case with (r = 1) gives the highest values of *Kx** while it appears from fig. 4-ii that the peak values of *Kx** occured at a value of (r) between 0.33 and 0.66.

It can be noticed from fig. 2 through fig. 4 that there are peak low values in *Kx** that appear to be constant regardless the value of (a/b). This value will be referred to as Kx^*_{min} as it reflects the minimum buckling capacity of the plate regardless the value of (a/b).

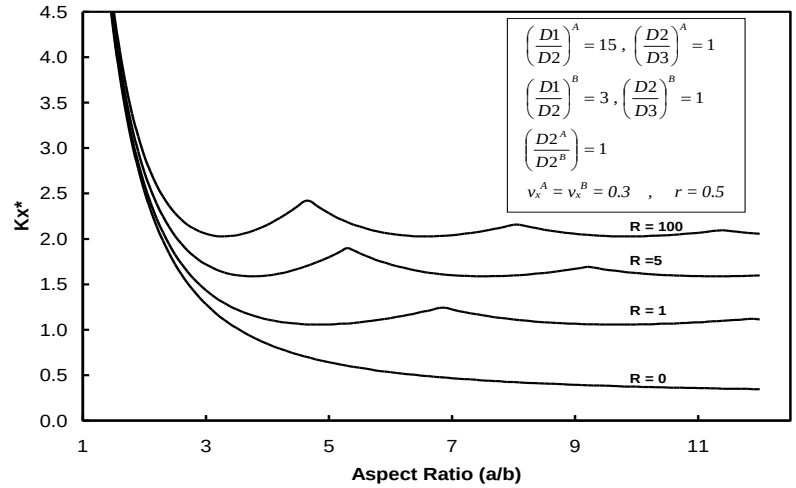

(a) Stiffer material at the free edge.

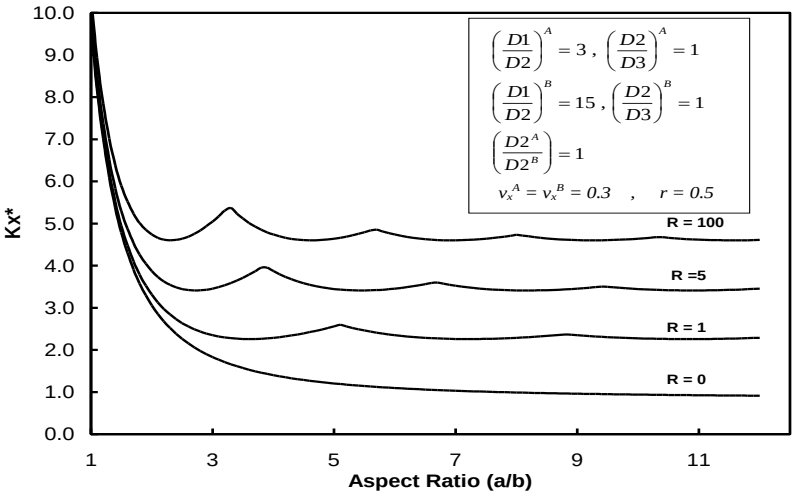

(b) Stiffer material at the rotationally restrained edge.

Fig. 2. Buckling curves for a hybrid plate for multiple values of R.

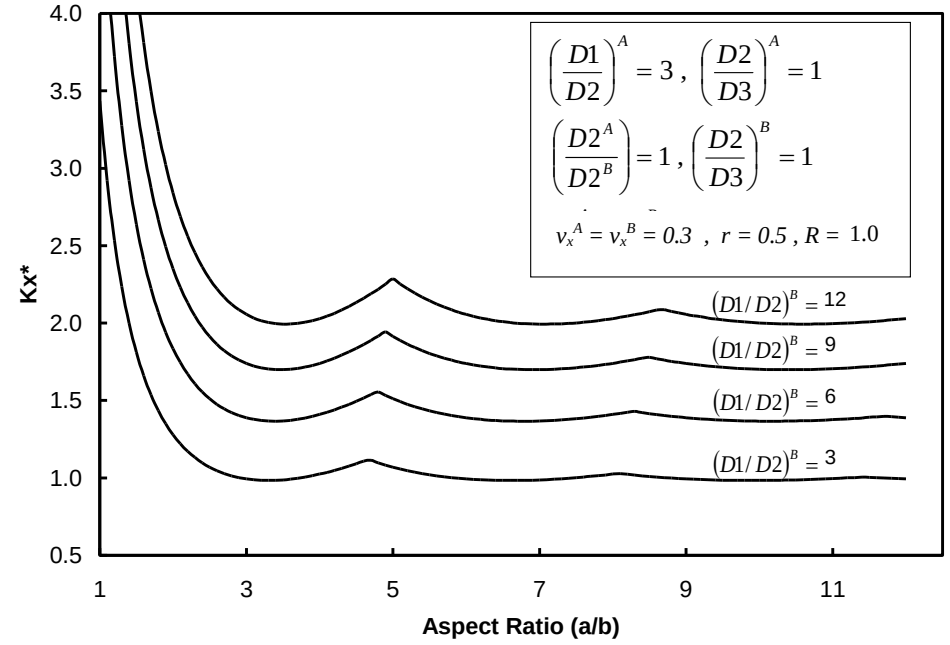

(a)

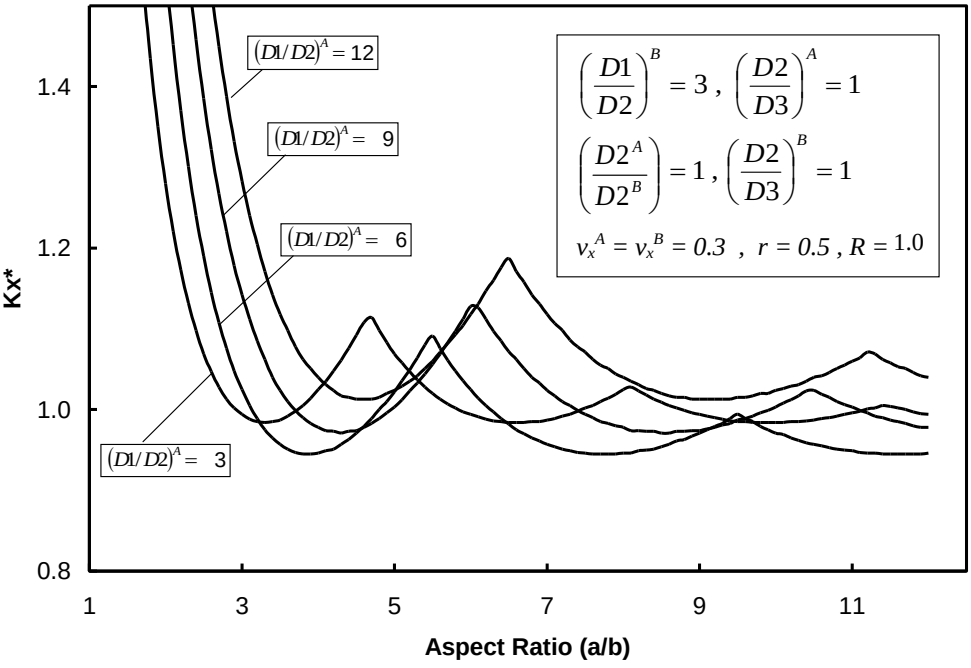

(b)

Fig. 3. Buckling curves for a hybrid plate (i) for multiple values of $(D1/D2)^B$ and (ii) for multiple values of $(D1/D2)^A$.

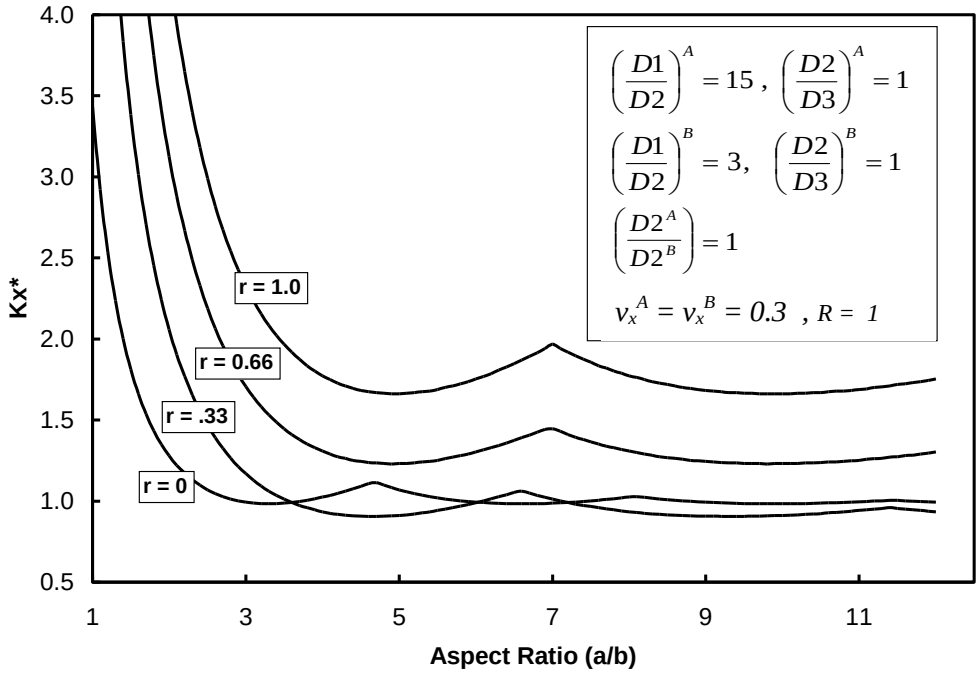

(a) Stiffer material at the free edge.

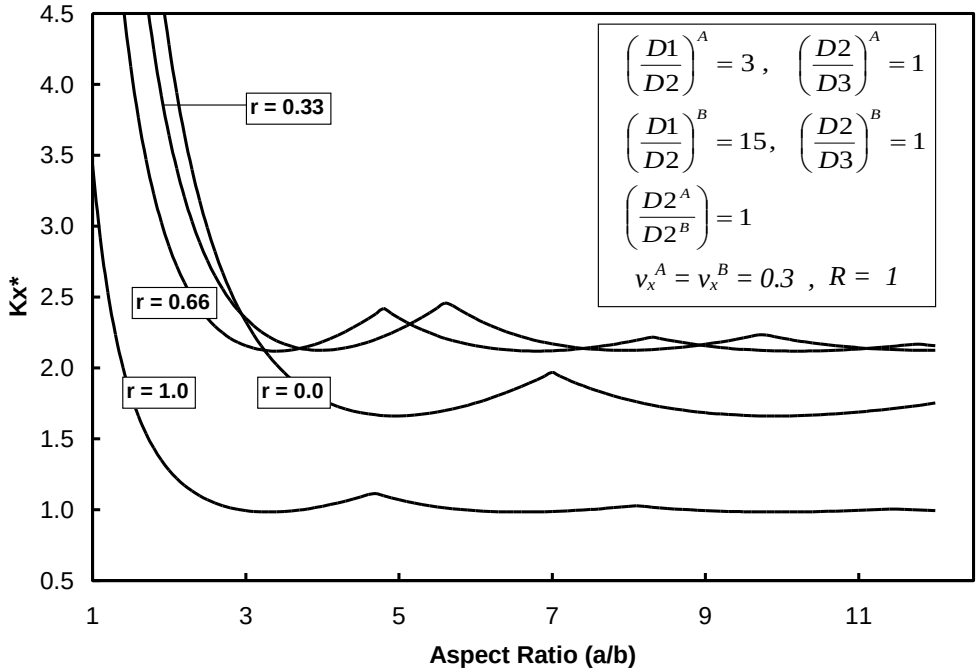

(b) Stiffer material at the rotationally restrained edge.

Fig. 4. Buckling curves for a hybrid plate for multiple values of *r*.

6.2. Influence of various parameters

In order to comprehensively investigate the effect of each of the parameters mentioned, they were plotted as an x-axis in fig. 5 through fig. 8 against the value of Kx^*_{min}. Fig. 5 and fig. 6 shows a plot of the width ratio (r) against the value of Kx^*_{min} for an isotropic and an orthotropic material cases, respectively. It is very clear from both figures that providing the stiffer material near the rotationally restrained edge generally provides higher buckling capacity to the plate than providing it near the free edge. It is important to notice that there was a peak high value of Kx^*_{min} that did not occur with the plate which is entirely made of the stiffer material. More important, there are certain values of (r) that may result in peak low values of Kx^*_{min} when the stiffer part is placed near the free edge of the plate. Fig. 7 shows that Kx^*_{min} generally decreases with the increase of $(D2^A/D2^B)$ except in cases with higher values of (r). It can be noticed from fig. 8 that Kx^*_{min} significantly increases with the increase of $(D1/D2)^B$ relative to $(D1/D2)^A$.

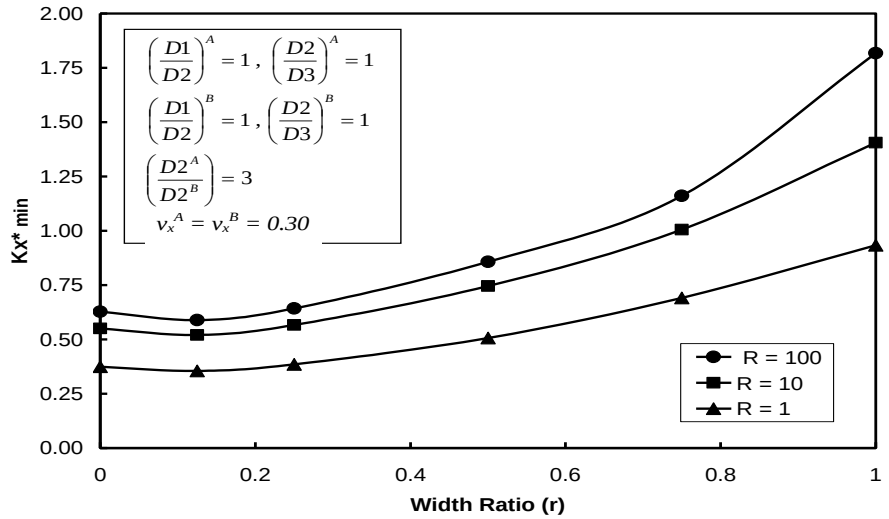

(a) Stiffer material at the free edge.

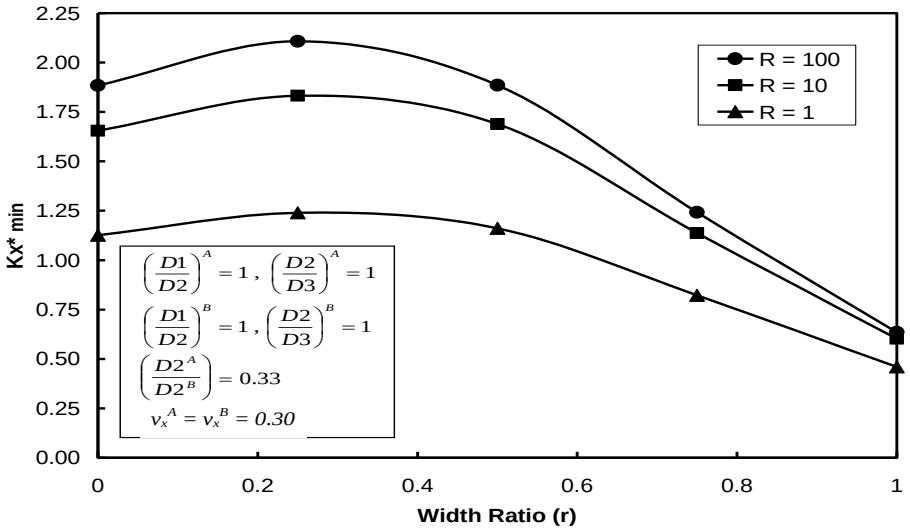

(b) Stiffer material at the rotationally restrained edge.

Fig. 5. Relation between Kx^*_{min} with the value of (r) for an isotropic material case.

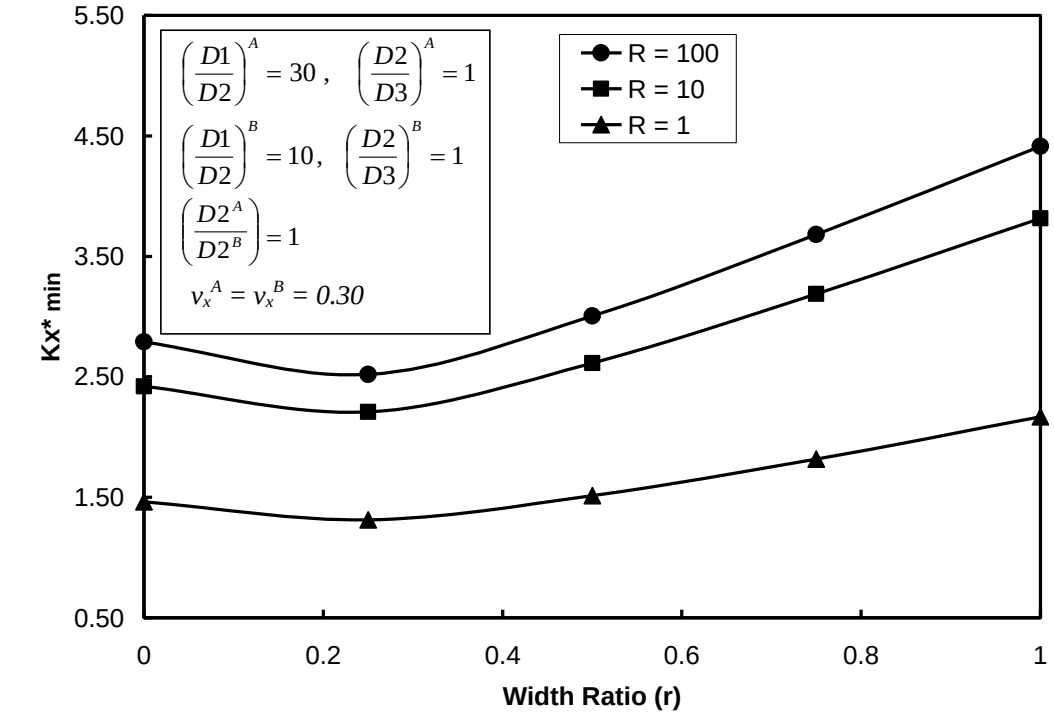

(a) Stiffer material at the free edge.

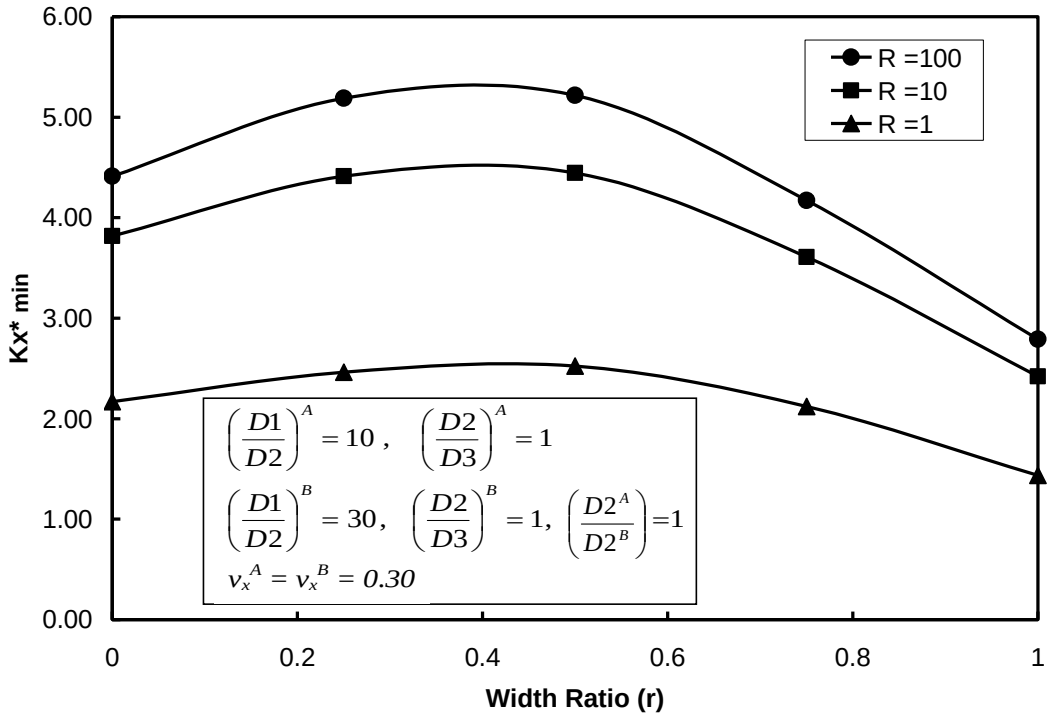

(b) Stiffer material at the rotationally restrained edge.

Fig. 6. Relation between Kx^*_{min} and the value of (r) for an orthotropic material case.

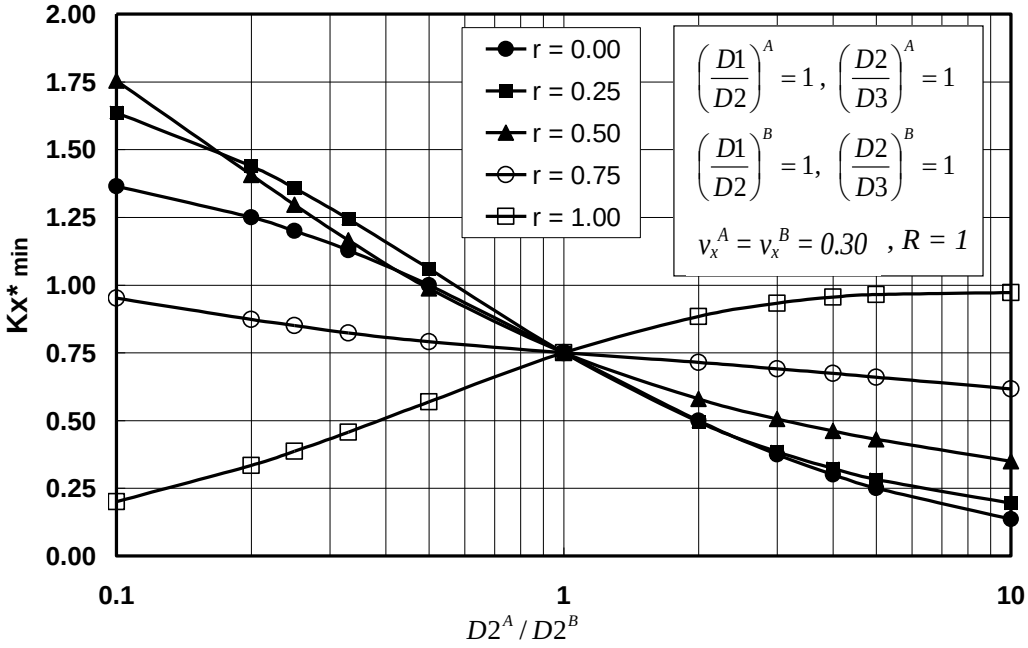

(a) Isotropic material.

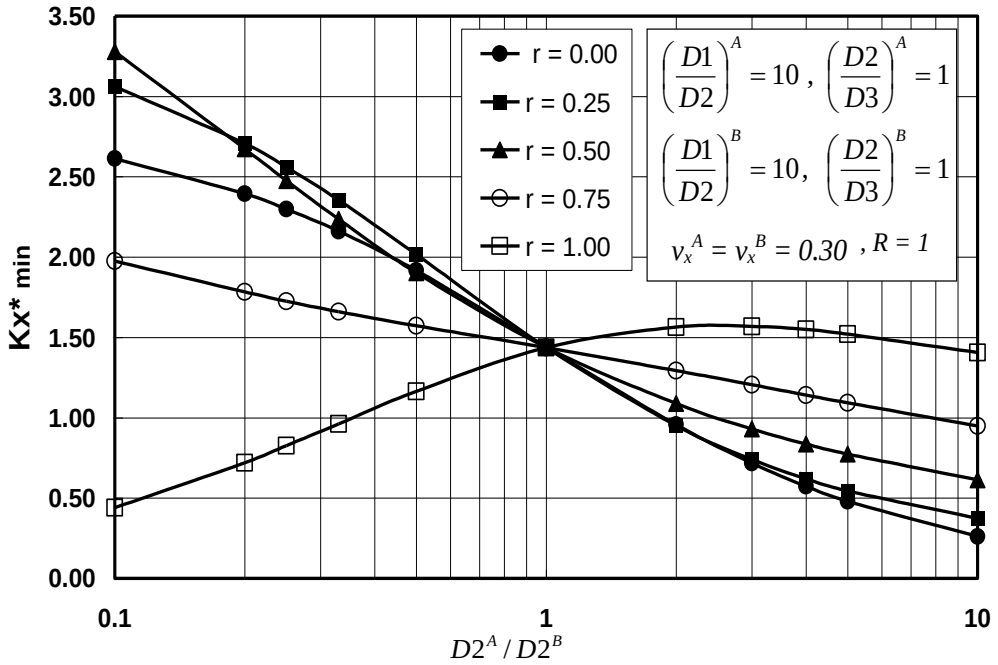

(b) Orthotropic material.

Fig. 7. Relation between Kx^*_{min} and the value of ($D2^A/D2^B$).

6.3. Application example

As an application example of the analytical model presented, a typical FRP plate that is a hybrid of glass and carbon fibers was studied using the analytical model presented. Two cases of plate hybridization were considered in the investigation see fig. 9. In the first case, the carbon fiber part was beside the free edge while it was beside the rotationally restrained edge in the other case. The properties of the materials of the plate were similar to those reported by Bank and Yin [10] and they are listed in table 1. In order to have a fair comparison between the two cases, the value of (*S.b*) were chosen to be identical in both cases. It is very clear from figure that providing the carbon fibers near the rotationally restrained edges resulted in a higher overall buckling capacity with a peak high value that typically occurred at a width ratio (*r*) of about 0.40.

7. Conclusions

An analytical model was presented for the buckling of an orthotropic plate that is a hybrid of two materials. The plate was considered to be subjected to uniaxial uniform strain loading and was considered to be simply supported at the loaded edges while it was free at one of the unloaded edges and rotationally restrained at the other one. A parametric study was presented to investigate the influence of each of the parameters of the problem. The study results showed that providing a stiffer material part near the rotationally restrained edge generally provides higher overall buckling capacity than providing it near the free edge. The peak high in plate buckling capacity does not occur with the plate totally made of the stiffer material. Providing the plate with a stiffer material at its edge might result in a decrease in its buckling capacity.

Table 1
Typical properties of FRP materials used in analysis

Property	Glass FRP	Carbon FRP
E_x (*GPa*)	17.24	181
E_y (*GPa*)	6.90	10.8
G (*GPa*)	2.93	7.17
υ_x	0.30	0.28

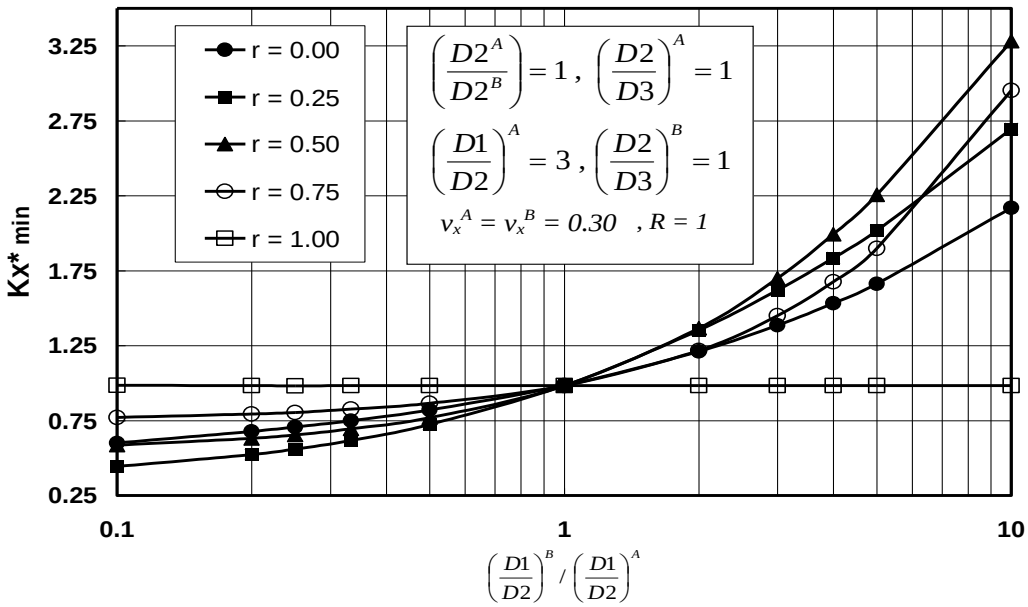

Fig. 8. Relation between Kx^*_{min} and $\left(\frac{D1}{D2}\right)^B / \left(\frac{D1}{D2}\right)^A$.

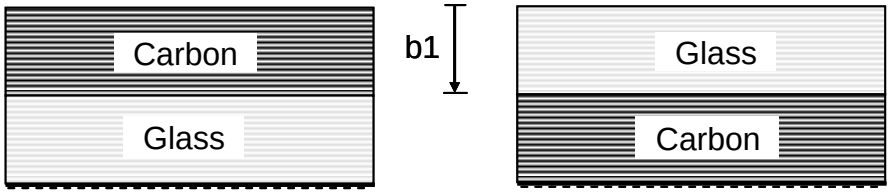

(a)

Case 1 **Case 2**

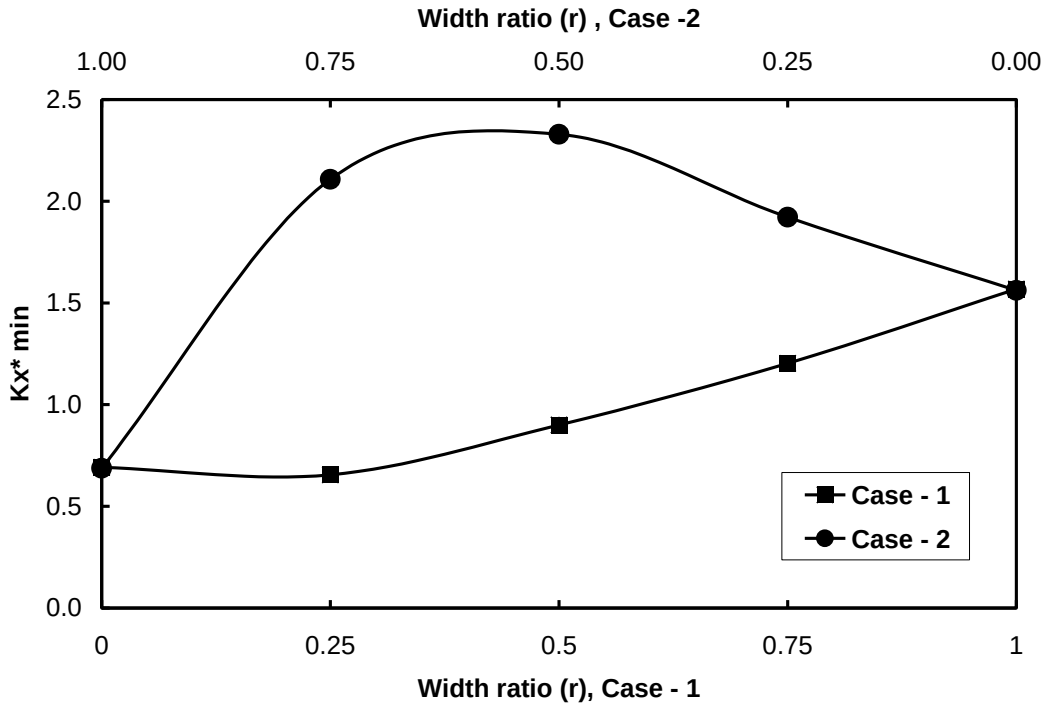

(b)

Fig. 9. Results of a hybrid FRP Carbon/Glass fiber plate.

Appendix I.

The equations listed below resulted from substituting with eqs. (30 and 31) into the boundary conditions related to the y-coordinates of the plate, i.e., eqs. (20 through 27). These equations are in terms of the constants *C*1 through *C*8:

$$1- \quad \left[(\lambda 1A)^2 - \upsilon_x{}^A.\left(\frac{b}{a}\right)^2 m^2\pi^2\right]C1+\left[(\lambda 1A)^2 - \upsilon_x{}^A.\left(\frac{b}{a}\right)^2 m^2\pi^2\right]C2+\left[-(\lambda 2A)^2 - \upsilon_x{}^A\left(\frac{b}{a}\right)^2 m^2\pi^2\right]C4=0 \qquad \text{(I-1)}$$

$$2- \quad \left[(\lambda 1A)^3 - \lambda 1A.\left(2\frac{D3^A}{D2^A} - {\upsilon_x}^A\right)\left(\frac{b}{a}\right)^2 m^2\pi^2\right] C1 + \left[-(\lambda 1A)^3 + \lambda 1A.\left(2\frac{D3^A}{D2^A} - {\upsilon_x}^A\right)\left(\frac{b}{a}\right)^2 m^2\pi^2\right] C2 + \left[-(\lambda 2A)^3 - \lambda 2A.\left(2\frac{D3^A}{D2^A} - {\upsilon_x}^A\right)\left(\frac{b}{a}\right)^2 m^2\pi^2\right] C3 = 0 \tag{I-2}$$

$$3- \quad \left(e^{\lambda 1B}\right).C5 + \left(e^{-\lambda 1B}\right).C6 + \sin(\lambda 2B).C7 + \cos(\lambda 2B).C8 = 0 \tag{I-3}$$

$$4- \quad \left((\lambda 1B)^2.\ e^{\lambda 1B} + R.\ \lambda 1B.\ e^{\lambda 1B}\right) C5 + \left((\lambda 1B)^2.\ e^{-\lambda 1B} - R.\ \lambda 1B.\ e^{-\lambda 1B}\right) C6 + \left[-(\lambda 2B)^2 \sin(\lambda 2B) + R.\lambda 2B.\cos(\lambda 2B)\right] C7 + \left[-(\lambda 2B)^2 \cos(\lambda 2B) - R.\lambda 2B.\sin(\lambda 2B)\right] C8 = 0 \tag{I-4}$$

$$5- \quad \left[e^{r.\lambda 1A}\right] C1 + \left[e^{-r.\lambda 1A}\right] C2 + [\sin(\lambda 2A.\ r)] C3 + [\cos(\lambda 2A.\ r)] C4 - \left[e^{r.\lambda 1B}\right] C5 - \left[e^{-r.\lambda 1B}\right] C6 - [\sin(\lambda 2B.\ r)] C7 - [\cos(\lambda 2B.\ r)] C8 = 0 \tag{I-5}$$

$$6- \quad \left[\left(\frac{D2^A}{D2^B}\right).(\lambda 1A)^2.\left(e^{\ r.\lambda 1A}\right) + K1\left(e^{r.\lambda 1A}\right)\right] C1 + \left[\left(\frac{D2^A}{D2^B}\right).(\lambda 1A)^2.\left(e^{-r.\lambda 1A}\right) + K1\left(e^{-r.\lambda 1A}\right)\right] C2 + \left[-\left(\frac{D2^A}{D2^B}\right).(\lambda 2A)^2 \sin(\lambda 2A.\ r) + K1.\sin(\lambda 2A.\ r)\right] C3 + \left[-\left(\frac{D2^A}{D2^B}\right).(\lambda 2A)^2 \cos(\lambda 2A.\ r) + K1.\cos(\lambda 2A.\ r)\right] C4 - \left[(\lambda 1B)^2.\left(e^{r.\ \lambda 1B}\right)^2 + K2.\left(e^{r.\ \lambda 1B}\right)\right] C5 - \left[(\lambda 1B)^2.\left(e^{-r.\ \lambda 1B}\right)^2 + K2.\left(e^{-r.\ \lambda 1B}\right)\right] C6 - \left[-(\lambda 2B)^2 \sin(\lambda 2B.\ r) + K2.\sin(\lambda 2B.\ r)\right] C7 - \left[-(\lambda 2B)^2 \cos(\lambda 2B.\ r) + K2.\cos(\lambda 2B.\ r)\right] C8 = 0 \tag{I-6}$$

Where,

$$K1 = \left(\frac{D2^A}{D2^B}\right).{\upsilon_x}^A.\left(\frac{b}{a}\right)^2 (-m^2\pi^2)$$

$$K2 = {\upsilon_x}^B.\left(\frac{b}{a}\right)^2 (-m^2\pi^2)$$

$$7- \quad \left[\left(\frac{D2^A}{D2^B}\right)(\lambda 1A)^3.e^{r.\lambda 1A} + K3.(\lambda 1A).e^{r.\lambda 1A}\right] C1 + \left[-\left(\frac{D2^A}{D2^B}\right)(\lambda 1A)^3.e^{-r.\lambda 1A} - K3.(\lambda 1A).e^{-r.\lambda 1A}\right] C2 + \left[-\left(\frac{D2^A}{D2^B}\right)(\lambda 2A)^3.\cos\ (r.\ \lambda 2A) + K3.(\lambda 2A).\cos\ (r.\ \lambda 2A)\right] C3 + \left[\left(\frac{D2^A}{D2^B}\right)(\lambda 2A)^3.\sin\ (r.\ \lambda 2A) - K3.(\lambda 2A).\sin\ (r.\ \lambda 2A)\right] C4 - \left[(\lambda 1B)^3.e^{r.\lambda 1B} + K4.(\lambda 1A).e^{r.\lambda 1B}\right] C5 - \left[-(\lambda 1B)^3.e^{-r.\lambda 1B} - K4.(\lambda 1A).e^{-r.\lambda 1B}\right] C6 - \left[-(\lambda 2B)^3.\cos\ (r.\ \lambda 2B) + K4.(\lambda 2B).\cos\ (r.\ \lambda 2B)\right] C7 - \left[(\lambda 2B)^3.\sin\ (r.\ \lambda 2B) - K4.(\lambda 2B).\sin\ (r.\ \lambda 2B)\right] C8 = 0 \tag{I-7}$$

where

$$K3 = \left(2\left(\frac{D3^A}{D2^A}\right)\left(\frac{D2^A}{D2^B}\right) - {\upsilon_x}^A.\left(\frac{D2^A}{D2^B}\right)\right)\left(\frac{b}{a}\right)^2 (-m^2\pi^2)$$

$$K4 = \left(2\left(\frac{D3^B}{D2^B}\right) - \upsilon_x{}^B\right) \cdot \left(\frac{b}{a}\right)^2 (-m^2\,\pi^2)$$

$$8- \quad \begin{aligned} &\left[\lambda 1A \cdot e^{r\,\cdot\,\lambda 1A}\right]C1 - \left[\lambda 1A \cdot e^{-r\,\cdot\,\lambda 1A}\right]C2 + \left[\lambda 2A \cdot \cos(r \cdot \lambda 2A)\right]C3 - \left[\lambda 2A \cdot \sin(r \cdot \lambda 2A)\right]C4 \\ &- \left[\lambda 1B \cdot e^{r\,\cdot\,\lambda 1B}\right]C5 + \left[\lambda 1B \cdot e^{-r\,\cdot\,\lambda 1B}\right]C6 - \left[\lambda 2B \cdot \cos(r \cdot \lambda 2B)\right]C7 + \left[\lambda 2B \cdot \sin(r \cdot \lambda 2B)\right]C8 = 0 \end{aligned} \qquad \text{(I-8)}$$

References

[1] "Creative Pultrusions Design Guide", Creative Pultrusions, Inc., Alum Bank, PA (2007).

[2] L.C. Bank, J. Yin and M. Nadipelli, "Local Buckling of Pultruded Beams-Nonlinearity, Anisotropy and Inhomogeneity", Construction and Building Materials, Vol. 9 (6), pp. 325-331(1995).

[3] P. Qiao and G. Zou, "Local Buckling of Composite Fiber-Reinforced Plastic Wide-Flange Sections", Journal of Structural Engineering, Vol. 129 (1), pp. 125-129 (2003).

[4] L.P. Kollar, "Local Buckling of Fiber Reinforced Plastic Composite Structural Members with Open and Closed Cross Sections", Journal of Structural Engineering, Vol. 129 (11), pp. 1503-1513 (2003).

[5] S.P. Timoshenko and J.M. Gere, Theory of Elastic Stability, 2nd Ed., McGraw-Hill Book Company, Inc., New York (1961).

[6] R.M. Jones, Mechanics of Composite Materials, Scripta Book Co., Washington (1975).

[7] E.J. Brunelle and G.A. Oyibo, "Generic Buckling Curves for Specially Orthotropic Rectangular Plates", AIAA Journal, Vol. 21 (8), pp. 1150-1156 (1983).

[8] J.M. Whitney, "Structural Analysis of Laminated Anisotropic Plates", Technomic Publishing, Lancaster, PA (1987).

[9] G. Bao, W. Jiang and J.C. Roberts, "Analytic and Finite Element Solutions for Bending and Buckling of Orthotropic Rectangular Plates", International Journal Solids Structures, Vol. 34 (14), pp. 1797-1822 (1997).

[10] L.C. Bank and J. Yin, "Buckling of Orthotropic Plates with Free and Rotationally Restrained Unloaded Edges," Thin-Walled Structures, Vol. 24 (1), pp. 83-96 (1996).

[11] C. Mittelstedt, "Closed-Form Analysis of the Buckling Loads of Symmetrically Laminated Orthotropic Plates Considering Elastic Edge Restraints", Composite Structures, Vol. 81 (4), pp. 550-558 (2007).

Received March 15, 2009
Accepted May 24, 2009